# Identification of Self-Excited Systems Using Discrete-Time, Time-Delayed Lur'e Models

Juan Paredes and Dennis S. Bernstein

Abstract—This paper considers system identification for systems whose output is asymptotically periodic under constant inputs. The model used for system identification is a discrete-time Lur'e model consisting of asymptotically stable linear dynamics, a time delay, a washout filter, and a static nonlinear feedback mapping. For sufficiently large scaling of the loop transfer function, these components cause divergence under small signal levels and decay under large signal amplitudes, thus producing an asymptotically oscillatory output. A least-squares technique is used to estimate the coefficients of the linear model as well as the parameters of a piecewise-linear approximation of the feedback mapping.

Index Terms—Self-excited oscillations; nonlinear feedback; system identification; discrete-time systems; least squares

#### I. INTRODUCTION

Nonlinear system identification is an exciting area of research with numerous challenges and open problems; the overview in [1] describes the status of the field and provides extensive references. The present paper focuses on nonlinear system identification for systems whose response to a constant input is asymptotically oscillatory, for example, periodic or almost periodic; a system of this type is called a self-excited system (SES). A classical example of a SES is the second-order van der Pol oscillator, whose states converge to a limit cycle. A SES, however, may have an arbitrary number of states and need not possess a limit cycle. Overviews of SES are given in [2], [3]; applications to chemical and biochemical systems are discussed in [4], [5]; self-excited thermoacoustic oscillation is discussed in [6], [7]; and fluidstructure interaction and its role in aircraft wing flutter is discussed in [8], [9]. These diverse applications show the rich appearance of SES in engineering and science.

A convenient model for SES is a feedback loop consisting of linear dynamics and a static nonlinear feedback mapping; a system of this type is called a *Lur'e system* [10]. Within the context of SES, Lur'e models are considered in [3], [11], [12], [13], [14], [15]. These works show that Lur'e models provide a flexible framework for modeling SES. The focus of the present paper is on discrete-time Lur'e models for SES; self-oscillating discrete-time systems are considered in [16], [17], [18]. The present paper appears to be the first to consider identification of SES using discrete-time Lur'e models.

As discussed in [19], [20], self-excited oscillations arise in Lur'e systems from a combination of stabilizing and destabilizing effects. In particular, the present paper considers a

Juan Paredes and Dennis S. Bernstein are with the Department of Aerospace Engineering, University of Michigan, Ann Arbor, MI, USA. {jparedes, dsbaero}@umich.edu

discrete-time, time-delay Lur'e model consisting of asymptotically stable linear dynamics, a time delay, a washout filter, and a static nonlinear feedback mapping. For all sufficiently large scalings of the loop transfer function, these components cause divergence under small signal levels and decay under large signal amplitudes, thus producing an asymptotically oscillatory output. A bias-generation mechanism is used to provide a nonzero offset in the oscillation. Similar features appear in [3], [11], [21].

The contribution of the present paper is the development of a nonlinear least-squares identification algorithm based on [22] as well as a numerical investigation of this technique for identifying SES using discrete-time, time-delayed Lur'e models. In setting up the model structure, the user must choose the order of the linear discrete-time dynamics and the number of steps delay. Once these are chosen, the system identification method estimates the parameters of the linear discrete-time dynamics as well as the static nonlinear feedback mapping, which is formulated as a continuous, piecewise-linear (CPL) function characterized by its slope in each interval of a user-chosen partition of the real line.

The contents of the paper are as follows. Section II introduces SES and the DTTDL model used for identification. Section III describes the parameterization of the CPL functions used to approximate the nonlinear feedback mapping. Section IV presents the DTTDL/CPL model, which consists of the DTTDL model with the CPL mapping parameterized in Section III. Section V describes the least-squares technique for identifying SES using DTTDL/CPL, and Section VI describes a variation of this technique for the constantinput case. Section VII presents numerical examples. Finally, Section VIII presents conclusions and future work.

**Notation.** 
$$\mathbb{R} \stackrel{\triangle}{=} (-\infty, \infty), \ \mathbb{N} \stackrel{\triangle}{=} \{0, 1, 2, \ldots\}.$$

# II. MODELING SELF-EXCITED SYSTEMS USING DISCRETE-TIME, TIME-DELAYED LUR'E MODELS

Let  $\mathcal S$  be a discrete-time, self-excited system (SES) with input v and output y, and let  $\mathcal M$  be a discrete-time model with input v and output  $y_{\mathrm m}$  (see Figure 1). The signals  $v,y,y_{\mathrm m}$  are scalar. The structure of  $\mathcal M$  is designed to capture the self-excited dynamics of  $\mathcal S$  in the sense that, for all sufficiently large constant v, there exist a nonconstant periodic function  $\tau\colon \mathbb N\to \mathbb R$  and  $k_0\in \mathbb N$  such that  $\lim_{k\to\infty}|y_k-\tau_k|=0$  and  $\lim_{k\to\infty}|y_{\mathrm m,k}-\tau_{k+k_0}|=0$ . In the case where  $\mathcal S$  is a continuous-time SES, the output  $y_k$  represents a sampled value of y. In this paper,  $\mathcal M$  is chosen to be a discrete-time, time-delayed Lur'e model.

$$v \longrightarrow S \longrightarrow v \longrightarrow M \longrightarrow v_{m}$$

Fig. 1. Self-excited system  $\mathcal S$  with input v and output y, and model  $\mathcal M$  with input v and output  $y_{\mathrm{m}}$ . A system identification algorithm is used to construct a model  $\mathcal M$  that captures the dynamics of  $\mathcal S$ .

The discrete-time, time-delayed Lur'e (DTTDL) model shown in Figure 2 incorporates the *n*th-order, asymptotically stable, strictly proper linear dynamics

$$G(\mathbf{q}) = \frac{B(\mathbf{q})}{A(\mathbf{q})} = \frac{b_1 \mathbf{q}^{n-1} + \dots + b_n}{\mathbf{q}^n + a_1 \mathbf{q}^{n-1} + \dots + a_n},$$
 (1)

where  $\mathbf{q}$  is the forward-shift operator, the bias-generation mechanism

$$v_{\rm b} = (\beta + v_{\rm f})v,\tag{2}$$

the time delay  $G_{\rm d}({\bf q})={\bf q}^{-d},$  where  $d\geq 0,$  the washout filter

$$G_{\rm f}(\mathbf{q}) = \frac{\mathbf{q} - 1}{\mathbf{q}},\tag{3}$$

and the nonlinear function  $\mathcal{N} \colon \mathbb{R} \to \mathbb{R}$  written as

$$v_{f,k} = \mathcal{N}(y_{f,k}). \tag{4}$$

Using  $y_{m,k} = G(\mathbf{q})v_{b,k}$ , it follows that

$$A(\mathbf{q})y_{\mathrm{m},k} = B(\mathbf{q})v_{\mathrm{b},k}$$
  
=  $B(\mathbf{q})[\beta + \mathcal{N}(y_{\mathrm{f},k})]v_k,$  (5)

and thus, for all  $k \ge n + d + 1$ ,

$$y_{m,k} = (1 - A(\mathbf{q}))y_{m,k} + B(\mathbf{q})[\beta + \mathcal{N}(y_{f,k})]v_{k}$$

$$= -a_{1}y_{m,k-1} - \dots - a_{n}y_{m,k-n}$$

$$+ \beta(b_{1}v_{k-1} + \dots + b_{n}v_{k-n})$$

$$+ b_{1}\mathcal{N}(y_{f,k-1})v_{k-1} + \dots + b_{n}\mathcal{N}(y_{f,k-n})v_{k-n},$$
(6)

where

$$y_{f,k} = y_{m,k-d} - y_{m,k-d-1}$$
.

Note that the propagation of (6) depends on the initial output values  $y_{m,0}, \ldots, y_{m,n+d}$ .

In [19], [20],  $\mathcal{N}$  is assumed to be bounded, continuous, either nondecreasing or nonincreasing, and changes sign (positive to negative or vice versa) at zero; hence,  $\mathcal{N}(0)=0$ . Under these assumptions, if the input v is constant and sufficiently large, then the output  $y_{\rm m}$  is nonconstant and asymptotically oscillatory.

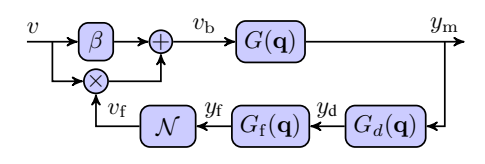


Fig. 2. Discrete-time, time-delayed Lur'e model with constant input  $\boldsymbol{v}$  and bias-generation mechanism.

### III. Parameterization of the continuous, piecewise-linear function ${\cal N}$

In this section, we assume that  $\mathcal{N}$  is continuous and piecewise-linear (CPL), and we parameterize  $\mathcal{N}$  as in [22]. Let  $c_1 < \cdots < c_p$ , let  $(-\infty, c_1], (c_1, c_2], \ldots, (c_{p-1}, c_p], (c_p, \infty)$  be a partition of the domain  $\mathbb{R}$  of  $\mathcal{N}$ , and define the vector

$$c \stackrel{\triangle}{=} [c_1 \cdots c_p]^{\mathrm{T}} \in \mathbb{R}^p.$$
 (7)

Furthermore, for all i = 1, ..., p+1, let  $\mu_i$  denote the slope of  $\mathcal{N}$  in the *i*th partition interval, and define the slope vector

$$\mu \stackrel{\triangle}{=} \left[ \mu_1 \cdots \mu_{p+1} \right]^{\mathrm{T}} \in \mathbb{R}^{p+1}. \tag{8}$$

Finally, letting  $\kappa \in \mathbb{R}$  and  $r \in \{1, \dots, p\}$ , it follows that, for all  $u \in \mathbb{R}$ ,  $\mathcal{N}$  can be written as

$$\mathcal{N}(u) = \mu^{\mathrm{T}} \eta(u) + \kappa, \tag{9}$$

where  $\eta \colon \mathbb{R} \to \mathbb{R}^{p+1}$  is defined by

$$\eta(u) \stackrel{\triangle}{=} \begin{cases} \eta_1(u), & \delta(u) < r+1, \\ \eta_2(u), & \delta(u) \ge r+1, \end{cases}$$
(10)

 $\delta(u) \in \{1, \dots, p+1\}$  is the index of the partition interval containing u, and

$$\eta_{1}(u) \stackrel{\triangle}{=} \begin{bmatrix} 0_{1 \times (\delta(u)-1)} & u - c_{\delta(u)} & c_{\delta(u)} - c_{\delta(u)+1} & \cdots \\ c_{r-1} - c_{r} & 0_{1 \times (p+1-r)} \end{bmatrix}^{T},$$
(11)

$$\eta_{2}(u) \stackrel{\triangle}{=} [0_{1 \times r} \ c_{r+1} - c_{r} \ \cdots \\ c_{\delta(u)-1} - c_{\delta(u)-2} \ u - c_{\delta(u)-1} \ 0_{1 \times (p+1-\delta(u))}]^{\mathrm{T}}.$$
(12)

Note that, in the case where  $\delta(u)=r$ , it follows from Eq. (11) that  $\eta_1(u)=\left[\begin{array}{ccc}0_{1\times(\delta(u)-1)}&u-c_{\delta(u)}&0_{1\times(p+1-r)}\end{array}\right]^T$ , whereas, in the case where  $\delta(u)=r+1$ , it follows from Eq. (12) that  $\eta_2(u)\stackrel{\triangle}{=}\left[\begin{array}{ccc}0_{1\times r}&u-c_{\delta(u)-1}&0_{1\times(p+1-\delta(u))}\end{array}\right]^T$ . Since  $\mathcal{N}(c_r)=\kappa$ , it can be seen that r and  $\kappa$  fix  $\mathcal{N}$  along the ordinate axis, as shown in Figure 3. Hence,  $\mathcal{N}$  is parameterized by c,  $\mu$ , r, and  $\kappa$ .

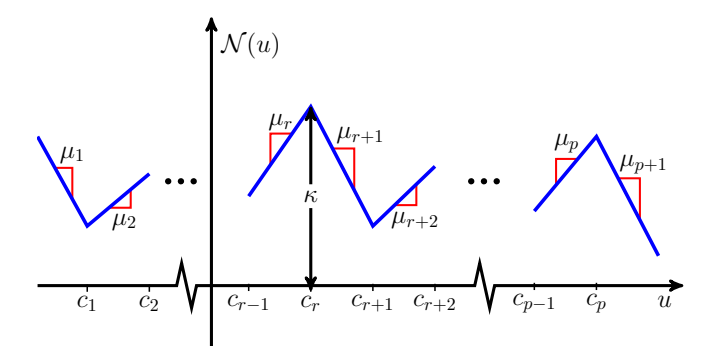


Fig. 3. Parameterization of the CPL function  $\mathcal N.$  Note that r and  $\kappa$  fix g along the ordinate axis.

## IV. DTTDL MODEL WITH A CPL NONLINEAR FEEDBACK MAPPING

In this section, we consider the DTTDL model in the case where  $\mathcal N$  is CPL; this is the DTTDL/CPL model. In order to enforce  $\mathcal N(0)=0$  (see Section II), we let  $\kappa=0$  and assume that, for some  $r,\,c_r=0$ . It thus follows from (6) and (9) that

$$y_{m,k} = -a_1 y_{m,k-1} - \dots - a_n y_{m,k-n} + \beta (b_1 v_{k-1} + \dots + b_n v_{k-n}) + b_1 \mu^{\mathrm{T}} \eta(y_{\mathrm{f},k-1}) v_{k-1} + \dots + b_n \mu^{\mathrm{T}} \eta(y_{\mathrm{f},k-n}) v_{k-n}.$$
(13)

Now, defining

$$a \stackrel{\triangle}{=} [a_1 \cdots a_n]^{\mathrm{T}}, \quad b \stackrel{\triangle}{=} [b_1 \cdots b_n]^{\mathrm{T}}, \quad (14)$$

it follows that (13) can be written as

$$y_{\mathrm{m},k} = \phi_k^{\mathrm{T}} \theta, \tag{15}$$

where

$$\theta \stackrel{\triangle}{=} \begin{bmatrix} a^{\mathrm{T}} & (\operatorname{vec}(\mu b^{\mathrm{T}}))^{\mathrm{T}} & \beta b^{\mathrm{T}} \end{bmatrix}^{\mathrm{T}},$$
 (16)

$$\phi_k \stackrel{\triangle}{=} \begin{bmatrix} -\phi_{y,k}^{\mathrm{T}} & \phi_{\eta,k}^{\mathrm{T}} & \phi_{v,k}^{\mathrm{T}} \end{bmatrix}^{\mathrm{T}}, \tag{17}$$

and

$$\phi_{y,k} \stackrel{\triangle}{=} \begin{bmatrix} y_{\mathrm{m},k-1} & \cdots & y_{\mathrm{m},k-n} \end{bmatrix}^{\mathrm{T}},$$
 (18)

$$\phi_{\eta,k} \stackrel{\triangle}{=} \begin{bmatrix} v_{k-1}\eta^{\mathrm{T}}(y_{\mathrm{f},k-1}) & \cdots & v_{k-n}\eta^{\mathrm{T}}(y_{\mathrm{f},k-n}) \end{bmatrix}^{\mathrm{T}}, (19)$$

$$\phi_{v,k} \stackrel{\triangle}{=} \begin{bmatrix} v_{k-1} & \cdots & v_{k-n} \end{bmatrix}^{\mathrm{T}}.$$
 (20)

### V. IDENTIFICATION OF DTTDL/CPL MODEL PARAMETERS

In this section, we present a least-squares identification technique for constructing a DTTDL/CPL model that approximates the response of the self-excited system  $\mathcal{S}$ . Since we do not assume that  $\mathcal{S}$  is a DTTDL system, the goal is to determine asymptotically stable  $\hat{G}$  and CPL  $\hat{\mathcal{N}}$  such that the response of the identified model  $\mathcal{M}$  approximates the response of the true system  $\mathcal{S}$ .

The least-squares identification technique depends on choosing values of n,d,c; these choices are denoted by  $\hat{n},\hat{d},\hat{c}$ . In practice,  $\hat{n},\hat{d},\hat{c}$  can be iteratively modified depending on the accuracy of the identification. The goal is thus to obtain parameter estimates  $\hat{a},\hat{b},\hat{\beta},\hat{\mu}$  for the DTTDL/CPL model. In the special case where  $\mathcal{S}$  is DTTDL or DTTDL/CPL, the parameters  $\hat{a},\hat{b},\hat{\beta},\hat{\mu}$  can be viewed as estimates of  $a,b,\beta,\mu$ .

Next, let  $l_{\rm u} \geq l_{\rm l} \geq \hat{n} + \hat{d} + 1$  and, for all  $k \in \{l_{\rm l} - \hat{n} - \hat{d} - 1, \ldots, l_{\rm u}\}$ , let  $v_k$  and  $y_k$  be the sampled measurements of  $\mathcal S$  used for identification. Then, define the least-squares cost

$$J(\theta) \stackrel{\triangle}{=} ||Y - \Phi\theta||_2, \tag{21}$$

where

$$Y \stackrel{\triangle}{=} \begin{bmatrix} y_{l_1} & \cdots & y_{l_{\mathbf{u}}} \end{bmatrix}^{\mathrm{T}}, \tag{22}$$

and

$$\Phi \stackrel{\triangle}{=} [ -\Phi_Y \quad \Phi_{\eta,Y} \quad \Phi_{V} ], \tag{23}$$

where

$$\Phi_{Y} \stackrel{\triangle}{=} \left[ \begin{array}{c} \phi_{Y,l_{1}}^{\mathrm{T}} \\ \vdots \\ \phi_{Y,l_{\mathrm{u}}}^{\mathrm{T}} \end{array} \right], \Phi_{\eta,Y} \stackrel{\triangle}{=} \left[ \begin{array}{c} \phi_{\eta,Y,l_{1}}^{\mathrm{T}} \\ \vdots \\ \phi_{\eta,Y,l_{\mathrm{u}}}^{\mathrm{T}} \end{array} \right], \Phi_{V} \stackrel{\triangle}{=} \left[ \begin{array}{c} \phi_{v,l_{1}}^{\mathrm{T}} \\ \vdots \\ \phi_{v,l_{\mathrm{u}}}^{\mathrm{T}} \end{array} \right],$$

and

$$\phi_{Y,k} \stackrel{\triangle}{=} \begin{bmatrix} y_{k-1} & \cdots & y_{k-\hat{n}} \end{bmatrix}^{\mathrm{T}}, \tag{25}$$

$$\phi_{\eta,Y,k} \stackrel{\triangle}{=} \begin{bmatrix} v_{k-1}\eta^{\mathrm{T}}(y_{\mathrm{f},Y,k-1}) & \cdots & v_{k-\hat{n}}\eta^{\mathrm{T}}(y_{\mathrm{f},Y,k-\hat{n}}) \end{bmatrix}^{\mathrm{T}},$$
(26)

$$y_{\mathbf{f},Y,k} \stackrel{\triangle}{=} y_{k-\hat{d}} - y_{k-\hat{d}-1}. \tag{27}$$

Since  $\theta$  given by (16) is not linear in  $b, \mu, \beta$ , we derive an upper bound for  $J(\theta)$ , which is subsequently minimized. To do this, let  $\theta_{\mathcal{A}} \in \mathbb{R}^{n(p+1)}$ , define  $\theta_{\Lambda} \stackrel{\triangle}{=} \beta b$ , and note that (22) can be written as

$$J(\theta) = ||Y - \Phi\theta + \Phi_{\eta,Y}\theta_{\mathcal{A}} - \Phi_{\eta,Y}\theta_{\mathcal{A}}||_{2}$$

$$= ||Y + \Phi_{Y}a - \Phi_{\eta,Y}\operatorname{vec}(\mu b^{\mathrm{T}})$$

$$- \Phi_{V}\theta_{\Lambda} + \Phi_{\eta,Y}\theta_{\mathcal{A}} - \Phi_{\eta,Y}\theta_{\mathcal{A}}||_{2}$$

$$= ||Y - \Phi\tilde{\theta} + \Phi_{\eta,Y}(\theta_{\mathcal{A}} - \operatorname{vec}(\mu b^{\mathrm{T}}))||_{2}, \qquad (28)$$

where

$$\tilde{\theta} \stackrel{\triangle}{=} \left[ \begin{array}{cc} a^{\mathrm{T}} & \theta_{\mathcal{A}}^{\mathrm{T}} & \theta_{\Lambda}^{\mathrm{T}} \end{array} \right]^{\mathrm{T}}.$$
 (29)

It follows from (28) that

$$J(\theta) \leq ||Y - \Phi\tilde{\theta}||_2 + ||\Phi_{\eta,Y}(\theta_{\mathcal{A}} - \operatorname{vec}(\mu b^{\mathrm{T}}))||_2$$
  

$$\leq ||Y - \Phi\tilde{\theta}||_2 + \sigma_{\max}(\Phi_{\eta,Y})||\theta_{\mathcal{A}} - \operatorname{vec}(\mu b^{\mathrm{T}})||_2$$
  

$$= J_{\mathrm{LS}}(\tilde{\theta}) + \sigma_{\max}(\Phi_{\eta,Y})J_{\mathcal{A}}(\theta_{\mathcal{A}}, \mu, b), \tag{30}$$

where

$$J_{\rm LS}(\tilde{\theta}) \stackrel{\triangle}{=} ||Y - \Phi \tilde{\theta}||_2, \tag{31}$$

$$J_{\mathcal{A}}(\theta_{\mathcal{A}}, \mu, b) \stackrel{\triangle}{=} ||\text{vec}^{-1}(\theta_{\mathcal{A}}) - \mu b^{\text{T}}||_{\text{F}},$$
 (32)

 $||\cdot||_{\rm F}$  denotes the Frobenius norm, and  $\sigma_{\rm max}$  denotes the largest singular value.

The upper bound for  $J(\theta)$  given by (30) is minimized by sequentially minimizing  $J_{LS}(\bar{\theta})$  and  $J_{A}(\theta_{A}, \mu, b)$  to obtain

$$\hat{\hat{\theta}} \stackrel{\triangle}{=} \underset{\bar{\theta}_0 \in \mathbb{R}^{n(p+3)}}{\operatorname{argmin}} J_{LS}(\bar{\theta}_0) = \begin{bmatrix} \hat{a}^{\mathrm{T}} & \hat{\theta}_{\mathcal{A}}^{\mathrm{T}} & \hat{\theta}_{\Lambda}^{\mathrm{T}} \end{bmatrix}^{\mathrm{T}}, \quad (33)$$

where  $\hat{\theta}_{\mathcal{A}} \in \mathbb{R}^{n(p+1)}$  and  $\hat{\theta}_{\Lambda} \stackrel{\triangle}{=} \hat{\beta}\hat{b}$ . Note that  $\hat{\theta}$  can be obtained by applying linear least-squares minimization to  $J_{\text{LS}}$ . Since  $\hat{\beta}$  and  $\hat{b}$  are unidentifiable from  $\hat{\theta}_{\Lambda}$ , choosing an arbitrary nonzero value for  $\hat{\beta}$  yields  $\hat{b} = \hat{\theta}_{\Lambda}/\hat{\beta}$ .

The following result is used to obtain  $\hat{\mu} = \underset{\mu_0 \in \mathbb{R}^{p+1}}{\operatorname{argmin}} J_{\mathcal{A}}(\hat{\theta}_{\mathcal{A}}, \mu_0, \hat{b}).$ 

Proposition 5.1: Let  $A \in \mathbb{R}^{n \times m}$ , let  $r \in \mathbb{R}^m$  be nonzero, and define  $V : \mathbb{R}^n \to \mathbb{R}$  by

$$V(x) \stackrel{\triangle}{=} ||A - xr^{\mathrm{T}}||_{\mathrm{F}}^{2}. \tag{34}$$

Then,

$$\underset{x \in \mathbb{R}^n}{\operatorname{argmin}} V(x) = (r^{\mathrm{T}}r)^{-1} A r. \tag{35}$$

**Proof.** For all  $x \in \mathbb{R}^n$ ,

$$V(x) = \text{tr}(A^{T}A) - 2x^{T}Ar + x^{T}xr^{T}r,$$
 (36)

and thus

$$V'(x) = -2Ar + 2r^{\mathrm{T}}rx, (37)$$

$$V''(x) = 2r^{\mathrm{T}}r > 0. {38}$$

It follows from (38) and [23, Theorem 3.3.8, p. 115] that V is strictly convex, which implies that V has at most one minimizer. Since

$$V'((r^{\mathrm{T}}r)^{-1}Ar) = 0, (39)$$

(38) implies that  $(r^{\mathrm{T}}r)^{-1}Ar$  is a local minimizer of V. Hence, [23, Theorem 3.4.2, pp. 125, 126] implies that  $(r^{\mathrm{T}}r)^{-1}Ar$  is the unique minimizer of V.

Proposition 5.1 implies that, for fixed  $\hat{\theta}_{\mathcal{A}}$  and  $\hat{b}$ , the value of  $\hat{\mu}$  that minimizes  $\hat{\mu} \mapsto J_{\mathcal{A}}(\hat{\theta}_{\mathcal{A}}, \hat{\mu}, \hat{b})$  is given by

$$\hat{\mu} = \frac{\text{vec}^{-1}(\hat{\theta}_{\mathcal{A}})\hat{b}}{\hat{b}^{\text{T}}\hat{b}}.$$
(40)

The identified DTTDL/CPL model  $\mathcal{M}$  is characterized by the chosen parameters  $\hat{n}, \hat{d}, \hat{c}, \hat{\beta}$ , as well as the estimated parameters  $\hat{a}, \hat{b}, \hat{\mu}$ . Note that multiplying  $\hat{\beta}$  by nonzero  $\gamma \in \mathbb{R}$  results in the division of  $\hat{b}$  by  $\gamma$  and the multiplication of  $\hat{\mu}$  by  $\gamma$ , which modifies the estimate of the nonlinear feedback mapping. However, it follows from (13) that the response of the identified model remains unchanged.

# VI. IDENTIFICATION OF DTTDL/CPL MODEL PARAMETERS WITH CONSTANT INPUT

This section considers a variation of the identification technique presented in the previous section for the case where v is constant, as typically occurs in self-excited systems. For  $v_k \equiv v_0$ , (13) becomes

$$y_{m,k} = -a_1 y_{m,k-1} - \dots - a_n y_{m,k-n} + \beta v_0 (b_1 + \dots + b_n)$$
  
+  $v_0 [b_1 \mu^T \eta(y_{f,k-1}) + \dots + b_n \mu^T \eta(y_{f,k-n})].$  (41)

Then, (41) can be expressed as (15), where

$$\theta \stackrel{\triangle}{=} \begin{bmatrix} a^{\mathrm{T}} & (\operatorname{vec}(\mu b^{\mathrm{T}})^{\mathrm{T}} & \beta \mathbf{1}_{1 \times n} b \end{bmatrix}^{\mathrm{T}},$$
 (42)

$$\phi_k \stackrel{\triangle}{=} \begin{bmatrix} -\phi_{y,k}^{\mathrm{T}} & \phi_{\eta,k}^{\mathrm{T}} & v_0 \end{bmatrix}^{\mathrm{T}}, \tag{43}$$

 $\phi_{y,k}$  is defined by (18), and where

$$\phi_{\eta,k} \stackrel{\triangle}{=} v_0 \left[ \eta^{\mathrm{T}}(y_{\mathrm{f},k-1}) \cdots \eta^{\mathrm{T}}(y_{\mathrm{f},k-n}) \right]^{\mathrm{T}}.$$
 (44)

Furthermore,  $J(\theta)$  can be written as in (21), where Y is defined by (22) and  $\Phi$  is defined by (23)–(27), where

$$\Phi_{\mathcal{V}} \stackrel{\triangle}{=} v_0 \mathbf{1}_{(l_{\mathcal{U}} - l_{\mathcal{U}} + 1) \times 1},\tag{45}$$

$$\phi_{\eta,Y,k} \stackrel{\triangle}{=} v_0 [\eta^{\mathrm{T}}(y_{\mathrm{f},Y,k-1}) \cdots \eta^{\mathrm{T}}(y_{\mathrm{f},Y,k-\hat{n}})]^{\mathrm{T}}.$$
 (46)

Since  $\theta$  given by (42) is not linear in  $b, \mu, \beta$ , we derive an upper bound for  $J(\theta)$ , which is subsequently minimized. Next, (21) can be rewritten as in (28), where  $\theta_{\mathcal{A}} \in \mathbb{R}^{n(p+1)}$ ,  $\theta_{\Lambda} \stackrel{\triangle}{=} \beta 1_{1 \times n} b$ , and  $\tilde{\theta}$  is defined as in (29). Then, an upper bound for  $J(\theta)$  can be derived as in (30), where  $J_{\mathrm{LS}}$  and  $J_{\mathcal{A}}$  are defined as in (31) and (32), and can be minimized by

sequentially minimizing  $J_{\rm LS}(\bar{\theta})$  and  $J_{\mathcal{A}}(\theta_{\mathcal{A}},\mu,b)$ . Let  $\hat{\theta}_{\mathcal{A}} \in \mathbb{R}^{n(p+1)}$ , define  $\hat{\theta}_{\Lambda} \stackrel{\triangle}{=} \hat{\beta}1_{1\times n}\hat{b}$ , and define  $\hat{\theta}$  as in (33). Then  $\hat{\theta}$  can be obtained by minimizing  $J_{\rm LS}$ .

Next, [24, Fact 11.16.39, p. 906] implies that, for fixed  $\hat{\theta}_{\mathcal{A}}$ , the rank-1 approximation of  $\hat{\mu}\hat{b}^{\mathrm{T}}$  that minimizes  $J_{\mathcal{A}}(\hat{\theta}_{\mathcal{A}},\hat{\mu},\hat{b})$  is given by

$$\hat{\mu}\hat{b}^{T} = \sigma_{\max}(\text{vec}^{-1}(\hat{\theta}_{A}))u_{A,1}v_{A,1}^{T}, \tag{47}$$

where  $\sigma_{\max}$  denotes the largest singular value,  $u_{\mathcal{A},1}$  denotes the first left-singular vector of  $\text{vec}^{-1}(\hat{\theta}_{\mathcal{A}})$ , and  $v_{\mathcal{A},1}$  denotes the first right-singular vector of  $\text{vec}^{-1}(\hat{\theta}_{\mathcal{A}})$ . Since  $\hat{\mu}$  and  $\hat{b}$  are unidentifiable from (47), choosing arbitrary nonzero  $\beta_{\text{LS}} \in \mathbb{R}$  and using it to separate (47) yields

$$\hat{\mu} = \beta_{LS} \ \sigma_{\max}(\text{vec}^{-1}(\hat{\theta}_{\mathcal{A}})) u_{\mathcal{A},1}, \quad \hat{b} = \frac{v_{\mathcal{A},1}}{\beta_{LS}}.$$
 (48)

Finally,  $\hat{\beta}$  is given by

$$\hat{\beta} = \frac{\hat{\theta}_{\Lambda}}{1_{1 \times \hat{n}} \hat{b}}.\tag{49}$$

The identified DTTDL/CPL model  $\mathcal{M}$  is characterized by the chosen parameters  $\hat{n}, \hat{d}, \beta_{\mathrm{LS}}$ , and  $\hat{c}$ , as well as the estimated parameters  $\hat{a}, \hat{b}, \ \hat{\beta}$  and  $\hat{\mu}$ . Note that multiplying  $\beta_{\mathrm{LS}}$  by nonzero  $\gamma \in \mathbb{R}$  results in the division of  $\hat{b}$  by  $\gamma$ , and the multiplication of  $\hat{\mu}$  (which scales  $\hat{\mathcal{N}}$ ) and  $\hat{\beta}$  by  $\gamma$ . However, it follows from (13) that the response of the identified model remains unchanged.

### VII. NUMERICAL EXAMPLES

In this section, we present numerical examples to illustrate identification of DTTDL/CPL models. Recursive least squares (RLS) is used for regression, as presented in [25], [26]. The identified systems include a DTTDL system (example VII-A), and a Van der Pol (VdP) system with output bias (example VII-B). For example VII-A, it is assumed that the input v is known. However, since example VII-B does not involve an external input, an arbitrary value of the input v is used to facilitate identification of the DTTDL model.

Example VII-A: DTTDL system with CPL, monotonic, odd  $\mathcal N$ 

Consider the DTTDL system S with  $\beta = 7.5$ , d = 4,

$$G(\mathbf{q}) = \frac{\mathbf{q} - 0.5}{\mathbf{q}^2 - 1.6\mathbf{q} + 0.8},\tag{50}$$

and the CPL, monotonic, odd feedback mapping  $\mathcal N$  shown in Figure 4. The domain of  $\mathcal N$  is partitioned by  $c=[-10\ -9\ \cdots\ 9\ 10\ ]^{\mathrm T}$ , and  $\mathcal N$  is constructed such that, for all  $i\in\{1,\ldots,21\}$ ,  $\mathcal N(c_i)=2.5\tanh(1.2c_i/2.5)$ . To obtain data for identification,  $y_0,\ldots,y_6$  are generated randomly, and, for all  $k\geq 0,\ v_k$  is a gaussian random variable with mean 5 and standard deviation  $\sqrt{1.5}$ . For all  $k\geq 7,\ y_k$  is generated by simulating  $\mathcal S$  with (50). The same technique is used in all subsequent examples.

For least-squares identification of the DTTDL/CPL model parameters, we let  $\hat{c}=c$  and  $\hat{\beta}=\beta$ , and we apply RLS with  $\theta_0=0,\,P_0=10^6$  and  $\lambda=1$  using data in [100,25000]. The

standard deviation of the sensor noise is chosen to be  $\sqrt{1.5}$ , which yields a measurement signal-to-noise ratio (SNR) of approximately 40 dB.

To assess the accuracy of the identified model, the input  $v_k \equiv 8$  is applied to the system  $\mathcal S$  with the initial conditions  $y_k = 300$  for all  $k \in [0,6]$ , as well as the identified model  $\mathcal M$  with the initial conditions  $y_{\mathrm{m},k} = 0$  for all  $k \in [0,6]$ . The response of the identified model based on noisy measurements with  $\hat n = 4$  and  $\hat d = d$  is shown in Figure 5. Figure 6 compares the power spectral density (PSD) of the output of  $\mathcal M$  for  $\hat n \in \{1,2,3\}$  and  $\hat d \in \{3,4,5\}$  obtained using noisy measurements with the PSD of the output of  $\mathcal S$ .

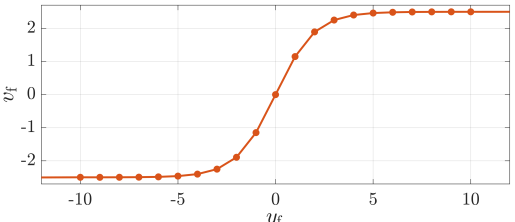


Fig. 4. Example VII-A: Piecewise-linear feedback mapping  $\mathcal{N}$ .

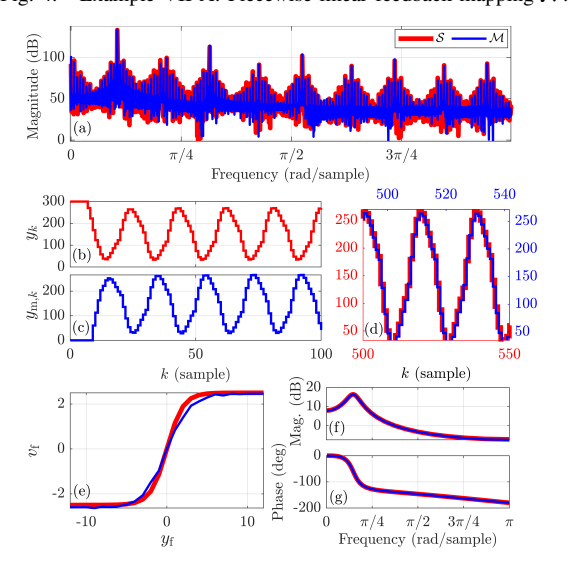


Fig. 5. Example VII-A: Least-squares identification of DTTDL/CPL model parameters using noisy measurements for  $\hat{n}=4$  and  $\hat{d}=d$ . (a) compares the PSD of the output of  $\mathcal{M}$  with the PSD of the output of  $\mathcal{S}$ . (b) shows the output of  $\mathcal{S}$  with  $v_k\equiv 8$  and with  $y_k=300$  for all  $k\in [0,6]$ . (c) shows the output of  $\mathcal{M}$  with  $v_k\equiv 8$  and with  $y_{m,k}=0$  for all  $k\in [0,6]$ . (d) shows the output of  $\mathcal{S}$  on [500,550] and the output of  $\mathcal{M}$  on [492,541]. (e) shows the true and estimated nonlinearities. (f) and (g) show the frequency responses of the linear dynamics of  $\mathcal{S}$  and  $\mathcal{M}$ .

Example VII-B: Van der Pol system with bias

Let the  $\ensuremath{\mathcal{S}}$  be the continuous-time Van der Pol system

$$\ddot{y} + \mu_0(y^2 - 1)\dot{y} + y = 0, (51)$$

where  $\mu_0$  is a constant parameter. Figure 7 represents S as a Lur'e system.

To obtain data for identification, let  $\mu_0=1$ , y(0)=0.1, and  $\dot{y}(0)=0$ . For all t>0, the Van der Pol system is simulated using ode45, and the output is sampled with sample time  $T_{\rm s}=0.1$  s. The integration accuracy of

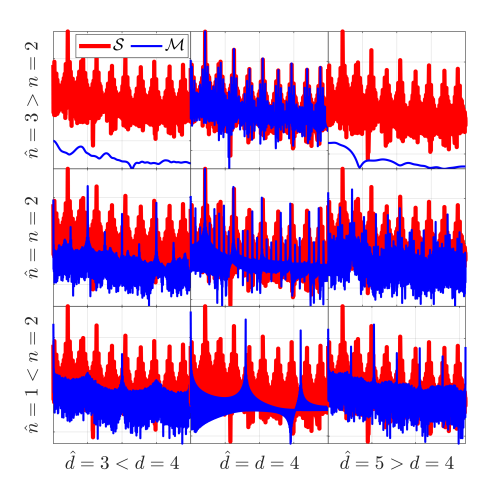


Fig. 6. Example VII-A: For  $\hat{n} \in \{1,2,3\}$  and  $\hat{d} \in \{3,4,5\}$ , these plots compare the PSD of the output of  $\mathcal{M}$  identified using noisy measurements with the PSD of the output of  $\mathcal{S}$ .

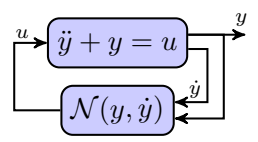


Fig. 7. Block representation of the Van der Pol system, where  $\mathcal{N}(y,\dot{y})=\mu_0(1-y^2)\dot{y}$ .

ode45 is set so that approximately 160 integration steps are implemented within each sample interval. A bias  $\bar{y}$  is added to all sampled measurements so that, for all  $k \geq 0$ , the biased output is  $y_k = y(kT_{\rm s}) + \bar{y}$ , where  $\bar{y} = 10$ . Finally, for identification purposes, it is assumed that  $v(t) \equiv 1$  is applied to  $\mathcal{S}$ .

For least-squares identification of the DTTDL/CPL model parameters with constant input, we let  $\hat{c}=[-0.3 \quad -0.275 \quad \cdots \quad 0.275 \quad 0.3 \ ]^{\mathrm{T}}, \, \hat{n}=12 \text{ and } \hat{d}=19,$  and  $\beta_{\mathrm{LS}}=-5,$  and we apply RLS with  $\theta_0=0, \, P_0=10^2$  and  $\lambda=1$  using data in [225,20000]. To assess the accuracy of the identified model,  $v_k\equiv 1$  is applied to the identified model  $\mathcal{M}$  with the initial conditions  $y_{\mathrm{m},k}=0$  for all  $k\in[0,31]$ . The response of the identified model based on noiseless measurements is shown in Figure 8.

Let  $\mathcal{S}_{\rm d}$  be the system whose output is the sampled output of  $\mathcal{S}$  and where the derivative of the sampled output is approximated by  $\dot{y}_k = \frac{y_{k+1} - y_{k-1}}{2T_{\rm s}}$ . Figure 9 compares the phase portraits of the continuous-time system  $\mathcal{S}$ , the discrete-time system  $\mathcal{S}_{\rm d}$ , and the identified model  $\mathcal{M}$  using  $\dot{y}_k = \frac{y_{k+1} - y_{k-1}}{2T_{\rm c}}$  to approximate the derivative of the output.  $\diamond$ 

### VIII. CONCLUSIONS AND FUTURE WORK

This paper developed a technique for identification of self-excited systems (SES) based on a discrete-time, time-delayed Lur'e (DTTDL) model. The nonlinear feedback mapping was chosen to be a continuous, piecewise-linear (CPL) function characterized by its slope in each interval of a user-chosen partition of the real line. By minimizing a bound on a nonquadratic cost function, linear least-squares techniques were used for parameter estimation within DTTDL/CPL.

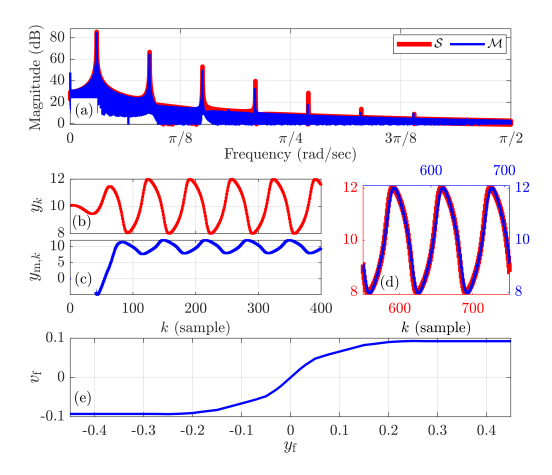


Fig. 8. Example VII-B: Least-squares identification of DTTDL/CPL model parameters for constant input measurements using noiseless measurements with  $\hat{n}=12$ ,  $\hat{d}=19$ , and  $\beta_{\rm LS}=-5$ . (a) compares the PSD of the output of  $\mathcal{M}$  with the PSD of the output of  $\mathcal{S}$ . (b) shows the biased sampled output of  $\mathcal{S}$ . (c) shows the output of the  $\mathcal{M}$  with  $v_k\equiv 1$  and  $y_{\rm m,k}=0$  for all  $k\leq 31$ . (d) shows the sampled output of  $\mathcal{S}$  on [550,750] and the output of  $\mathcal{M}$  on [508,708]. (e) shows the estimated nonlinear feedback mapping.

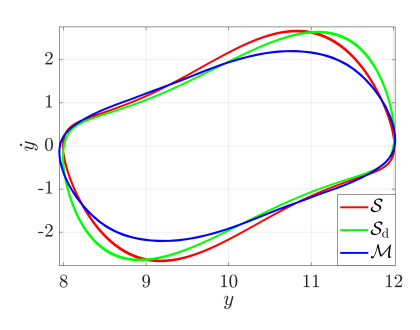


Fig. 9. Example VII-B: Phase portraits of the response of the continuous-time Van der Pol system  $\mathcal S$  with  $\mu_0=1$ , the response of the discrete-time system  $\mathcal S_{\rm d}$ , whose output is the sampled output of  $\mathcal S_{\rm d}$  and the response of the identified model  $\mathcal M$ . The derivative of the output of  $\mathcal S_{\rm d}$  and  $\mathcal M$  is approximated by using  $\dot y_k = \frac{y_k + 1 - y_k - 1}{2T_c}$ .

Numerical examples included both discrete-time and continuous-time systems with sampled data. Of particular interest was the ability of the DTTDL model to reproduce the limit-cycle response of the Van der Pol oscillator. Although this system does not have the structure of a DTTDL model, the system identification technique was able to approximately reproduce the phase-plane dynamics of this system.

Future research will focus on efficient techniques for determining the user-chosen partition of the real line needed to parameterize the static nonlinear feedback mapping. Finally, the numerical results motivate a fundamental research question, namely, to what extent can DTTDL/CPL models approximate the response of an arbitrary SES system.

### IX. ACKNOWLEDGMENTS

This research was supported by NSF grant CMMI 1634709, "A Diagnostic Modeling Methodology for Dual Retrospective Cost Adaptive Control of Complex Systems."

#### REFERENCES

- J. Schoukens and L. Ljung, "Nonlinear System Identification: A User-Oriented Road Map," *IEEE Contr. Sys.*, vol. 39, pp. 28–99, Dec. 2019.
- [2] A. Jenkins, "Self-oscillation," *Physics Reports*, vol. 525, no. 2, pp. 167–222, 2013.
- [3] W. Ding, Self-Excited Vibration: Theory, Paradigms, and Research Methods. Springer, 2010.
- [4] P. Gray and S. K. Scott, Chemical Oscillations and Instabilities: Nonlinear Chemical Kinetics. Oxford, 1990.
- [5] A. Goldbeter and M. J. Berridge, Biochemical Oscillations and Cellular Rhythms: The Molecular Bases of Periodic and Chaotic Behaviour. Cambridge, 1996.
- [6] A. P. Dowling, "Nonlinear Self-Excited Oscillations of a Ducted Flame," J. Fluid Mech., vol. 346, pp. 271–291, 1997.
- [7] Y. Chen and J. F. Driscoll, "A multi-chamber model of combustion instabilities and its assessment using kilohertz laser diagnostics in a gas turbine model combustor," *Combustion and Flame*, vol. 174, pp. 120–137, 2016.
- [8] R. D. Blevins, Flow-Induced Vibration. Van Nostrand Reinhold, 1990.
- [9] E. Jonsson, C. Riso, C. A. Lupp, C. E. S. Cesnik, J. R. R. A. Martins, and B. I. Epureanu, "Flutter and post-flutter constraints in aircraft design optimization," *Progress in Aerospace Sciences*, vol. 109, p. 100537, August 2019.
- [10] H. K. Khalil, Nonlinear Systems, 3rd ed. Prentice Hall, 2002.
- [11] D. H. Zanette, "Self-sustained oscillations with delayed velocity feedback," *Papers in Physics*, vol. 9, pp. 090 003–1–090 003–7, March 2017
- [12] S. Chatterjee, "Self-excited oscillation under nonlinear feedback with time-delay," *Journal of Sound and Vibration*, vol. 330, no. 9, pp. 1860– 1876, 2011.
- [13] G. Stan and R. Sepulchre, "Analysis of interconnected oscillators by dissipativity theory," *IEEE Transactions on Automatic Control*, vol. 52, no. 2, pp. 256–270, 2007.
- [14] A. Mees and L. Chua, "The Hopf bifurcation theorem and its applications to nonlinear oscillations in circuits and systems," *IEEE Transactions on Circuits and Systems*, vol. 26, no. 4, pp. 235–254, 1979.
- [15] L. T. Aguilar, I. Boiko, L. Fridman, and R. Iriarte, "Generating self-excited oscillations via two-relay controller," *IEEE Transactions on Automatic Control*, vol. 54, no. 2, pp. 416–420, 2009.
- [16] V. Rasvan, "Self-sustained oscillations in discrete-time nonlinear feed-back systems," in *Proc. 9th Mediterranean Electrotechnical Conference*, 1998, pp. 563–565.
- [17] M. B. D'Amico, J. L. Moiola, and E. E. Paolini, "Hopf bifurcation for maps: a frequency-domain approach," *IEEE Transactions on Circuits* and Systems I: Fundamental Theory and Applications, vol. 49, no. 3, pp. 281–288, March 2002.
- [18] F. S. Gentile, A. L. Bel, M. B. D'Amico, and J. L. Moiola, "Effect of delayed feedback on the dynamics of a scalar map via a frequencydomain approach," *Chaos: An Interdisciplinary Journal of Nonlinear Science*, vol. 21, no. 2, p. 023117, 2011.
- [19] J. Paredes, S. A. U. Islam, O. Kouba, and D. S. Bernstein, "A Discrete-Time, Time-Delayed Lur'e Model with Biased Self-Excited Oscillations," 2020, arXiv:2003.03420.
- [20] J. Paredes, S. A. U. Islam, and D. S. Bernstein, "A Time-Delayed Lur'e model with Biased Self-Excited Oscillations," in *Proc. Amer. Contr. Conf.*, Denver, July 2020, pp. 2699–2704.
- [21] S. Risau-Gusman, "Effects of time-delayed feedback on the properties of self-sustained oscillators," *Phys. Rev. E*, vol. 94, p. 042212, October 2016.
- [22] T. H. Van Pelt and D. S. Bernstein, "Non-linear system identification using Hammerstein and non-linear feedback models with piecewise linear static maps," *International Journal of Control*, vol. 74, no. 18, pp. 1807–1823, 2001.
- [23] M. S. Bazaraa, H. D. Sherali, and C. M. Shetty, Nonlinear programming theory and algorithms, 3rd ed. John Wiley & Sons, 2006.
- [24] D. S. Bernstein, Scalar, Vector, and Matrix Mathematics: Theory, Facts, and Formulas-Revised and Expanded Edition. Princeton University Press, 2018.
- [25] K. J. Astrom and B. Wittenmark, Adaptive Control, 2nd ed. Addison-Wesley, 1995.
- [26] S. A. U. Islam and D. S. Bernstein, "Recursive least squares for real-time implementation," *IEEE Control Systems Magazine*, vol. 39, no. 3, pp. 82–85, 2019.